JOURNAL OF THE KOREAN ASTRONOMICAL SOCIETY
43: 55 ~ 64, 2010 June

NON-HYDROSTATIC SUPPORT OF PLASMA IN THE SOLAR CHROMOSPHERE AND CORONA

JONGCHUL CHAE
Astronomy Program, Department of Physics and Astronomy, Seoul National University, Seoul 151-747, Korea
E-mail : jcchae@snu.ac.kr
(Received March 27, 2010; Accepted April 6, 2010)

ABSTRACT

We investigate how plasma structures in the solar chromosphere and corona can extend to altitudes much above hydrostatic scale heights from the solar surface even under the force of gravity. Using a simple modified form of equation of motion in the vertical direction, we argue that there are two extreme ways of non-hydrostatic support: dynamical support and magnetic support. If the vertical acceleration is downward and its magnitude is a significant fraction of gravitational acceleration, non-hydrostatic support is dynamical in nature. Otherwise non-hydrostatic support is static, and magnetic support by horizontal magnetic fields is the only other possibility. We describe what kind of observations are needed in the clarification of the nature of non-hydrostatic support. Observations available so far seem to indicate that spicules in the quiet regions and dynamic fibrils in active regions are dynamically supported whereas the general chromosphere as well as prominences is magnetically supported. Moreover, it appears that magnetic support is required for plasma in some coronal loops as well. We suspect that the identification of a coronal loop with a simple magnetic flux tube might be wrong in this regard.

Key words : magnetohydrodynamics (MHD) — Sun: atmosphere — Sun: chromosphere — Sun: corona

1. INTRODUCTION

A well-known, but little-understood property of the upper solar atmosphere — chromosphere and corona — is that it has a multitude of diverse plasma structures that extend to heights much above pressure scale heights expected in hydrostatic equilibrium. Spicules seen beyond the solar limb (see Fig. 1), for example, extend to as high as 7,000 km (Lippincott 1957; Pasachoff et al. 2009), which is far greater than a few hundred km, the hydrostatic pressure scale height of plasma in the chromosphere. The disk-counterpart of spicules is believed to be dark mottles in quiet regions. Fibrils usually seen in active regions are similar to, but are more elongated and less high than dark mottles. Fibrils have heights of about 4,000 km (Foukal 1971), which is still far greater than the hydrostatic pressure scale height. A similar situation arises even in the chromosphere itself seen beyond the limb which has a height of 5,000 km (Zirin 1996; Johannesson & Zirin 1996), and in solar prominences that lie much higher than spicules, fibrils, and any other chromospheric features (see Fig. 2).

Non-hydrostatic support seems to be needed even in some coronal loops emitting Extreme Ultraviolet (EUV) radiation (see Fig. 3). Aschwanden et al. (2000) determined pressure scale height in a number of EUV loops by analyzing intensity variation along each loop and found that long loops usually have pressure scale heights as large as three times hydrostatic pressure scale height. This means that the visible portion of a loop extends to a much higher altitude than is expected in a hydrostatic equilibrium as vividly illustrated by Aschwanden et al. (2001).

The non-hydrostatic support of plasma against gravity in the solar chromosphere and corona is a challenging problem as is the heating of the chromosphere and corona. These two problems may not be independent of each other, and solving the problem of non-hydrostatic support may be able to provide important clues to the problem of heating. To solve the problem of non-hydrostatic support, it is necessary to properly understand its nature from a general point of view, to consider probable solutions in each situation based on previous observations and to carry out new observations that can be used to discriminate among different possibilities. This kind of effort would be quite timely with the advent of new observing facilities with $0.2''$ or better resolving power that allow detailed comparison between theory and observation. This is the motivation of the present study.

2. PHYSICAL NATURE OF NON-HYDROSTATIC SUPPORT

2.1 Hydrostatic Support

A medium of plasma is in a hydrostatic equilibrium if it is static with the force of gravity being balanced by

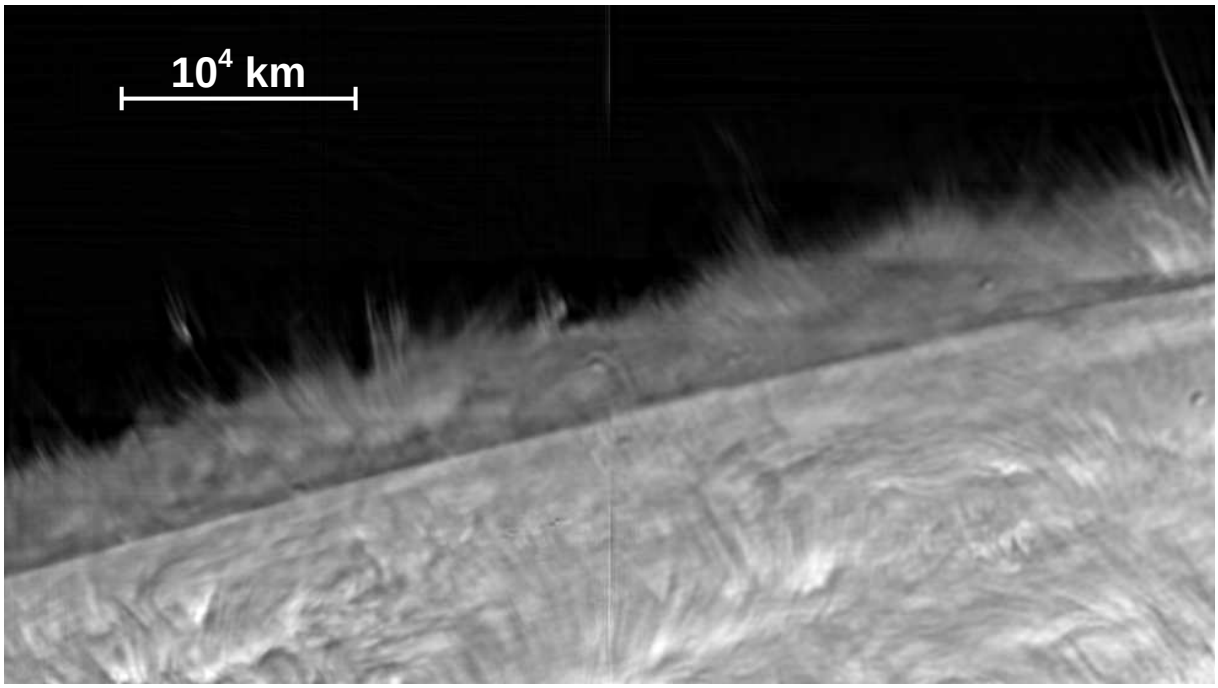

Fig. 1.— Solar chromosphere seen at the Hα centerline beyond the solar limb. The image was reconstructed from a set of short-exposure (speckle) images taken by the 1.6 m New Solar Telescope at Big Bear Solar Observatory. The spatial resolution is better than $0.2''$ or 150 km.

that of gas pressure gradient in the vertical direction:

$$\rho g = -\frac{\partial p}{\partial z}, \tag{1}$$

where p and ρ are pressure and mass density of plasma, g, gravitational acceleration, and z, vertical coordinate increasing in the upward direction. This condition has been commonly adopted for the study of stellar interiors and stellar photospheres. With pressure scale height

$$H_p \equiv -\left(\frac{\partial \ln p}{\partial z}\right)^{-1} \tag{2}$$

and hydrostatic scale height

$$H_s \equiv \frac{p}{\rho g}, \tag{3}$$

the condition of hydrostatic equilibrium may be simply expressed as

$$\frac{1}{H_s} = \frac{1}{H_p}, \tag{4}$$

which shows why pressure scale height and hydrostatic scale height are often regarded as the same. Note, however, that hydrostatic scale height refers to pressure scale height in a hydrostatic equilibrium, and in general these two scale heights do differ from each other. Pressure scale height H_p measures the actual extent of the medium of plasma or a structure of plasma in the vertical direction, whereas hydrostatic scale height H_s, the theoretical extent in a hydrostatic equilibrium. Note also that H_s is positive-definite, but H_p is not. With the help of the equation of state for an ideal gas, one can easily derive the following specific expression for H_s

$$H_s = 140 \left(\frac{T}{6000\ \mathrm{K}}\right)\left(\frac{1.3}{\mu}\right)\left(\frac{274\ \mathrm{m\ s^{-2}}}{g}\right)\ \mathrm{km}, \tag{5}$$

which indicates that H_s is determined by temperature T and mean molecular weight μ of the plasma as well as by g. Its value is estimated to be about 140 km in the photosphere with $T = 6,000$ K and $\mu = 1.3$, 240 km in the chromosphere with $T = 8,000$ K and $\mu = 1.0$, and 5×10^4 km in the corona with $T = 1 \times 10^6$ K and $\mu = 0.6$, respectively.

2.2 Non-Hydrostatic Support

Non-hydrostatic support is required when the force of plasma pressure gradient can not balance the force of gravity. This happens either when the magnitude of pressure gradient is too small or when its direction is reversed, that is, downward. The small pressure gradient means a tall extent of plasma ($H_p > H_s$), and the reverse direction of pressure gradient obviously refers to the existence of high-pressure features above low-pressure ones ($H_p < 0$). Both these cases are described by the inequality condition

$$\frac{1}{H_s} > \frac{1}{H_p}. \tag{6}$$

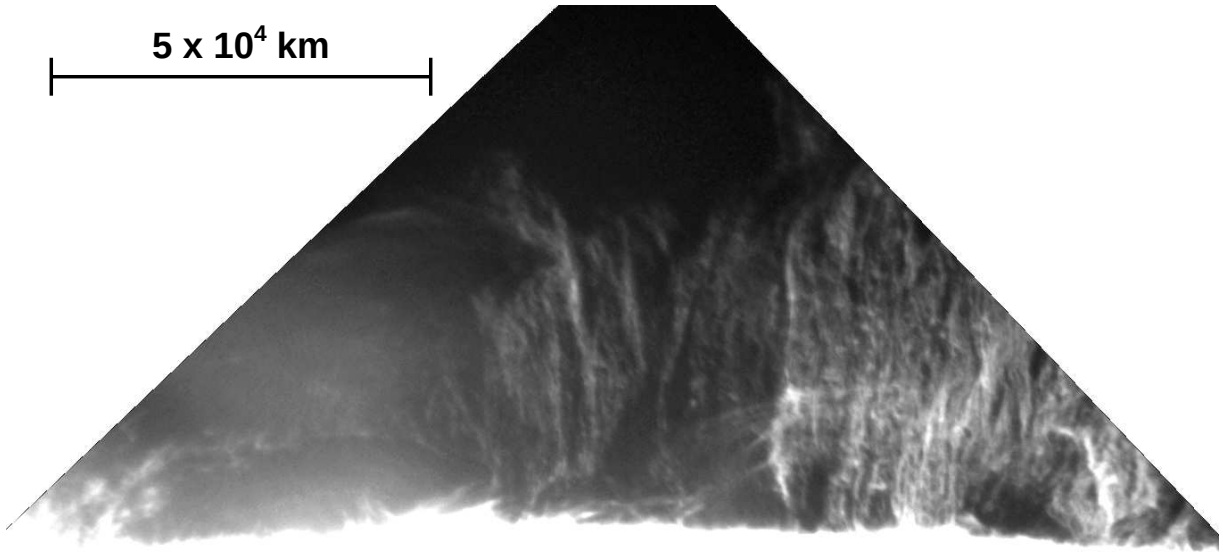

Fig. 2.— Hedgerow prominence seen at the Hα centerline. The image was taken by the Solar Optical Telescope aboard the *Hinode* satellite.

There exist two kinds of explanation for non-hydrostatic support: one is that there exist forces other than the force of plasma pressure gradient that can balance the force of gravity. As a matter of fact, the only other force that can exist in ideal MHD is the magnetic force or the Lorentz force. Therefore, non-hydrostatic support is magnetic in nature. The other is that the system may not be static at all: plasma may be moving under the force of gravity. This corresponds to the case of dynamical support. We fear that the terminology "dynamical support" might be misleading. The "support" used in the present work is not to imply the existence of some force balancing the force of gravity, but to generally refer to a mechanism or process to allow material to exist at high altitudes, including the case of force balance.

2.3 Magnetic Support

We assume that plasma in the solar chromosphere and corona may be treated as an inviscid single fluid where ideal magnetohydrodynamics (MHD) holds. Then in the presence of magnetic field $\boldsymbol{B}$, plasma carrying electric current is subject to another force: the Lorentz force

$$\boldsymbol{F}_L = \frac{1}{4\pi}(\nabla \times \boldsymbol{B}) \times \boldsymbol{B}\,. \tag{7}$$

Decomposing $\boldsymbol{B}$ into the vertical component and the horizontal component

$$\boldsymbol{B} = \hat{z}B_z + \boldsymbol{B}_h\,, \tag{8}$$

we can write the vertical component of the Lorentz force as

$$F_{L,z} = -\frac{1}{8\pi}\frac{\partial B_h^2}{\partial z} + \frac{1}{4\pi}\boldsymbol{B}_h \cdot \nabla B_z\,. \tag{9}$$

An important feature obvious from this equation is that horizontal magnetic field $\boldsymbol{B}_h$ is crucial for the non-zero vertical component of the Lorentz force, and hence for the magnetic support of non-hydrostatic plasma. This equation also indicates that, as is well known, the Lorenz force may be split into two parts: the force of magnetic pressure gradient and the force of magnetic tension.

A magnetohydrostatic equilibrium requires the balance among the force of gravity, the force of plasma pressure gradient, and the Lorentz force in the vertical direction:

$$\rho g = -\frac{\partial p}{\partial z} - \frac{1}{8\pi}\frac{\partial B_h^2}{\partial z} + \frac{1}{4\pi}\boldsymbol{B}_h \cdot \nabla B_z\,. \tag{10}$$

The last term in the right-hand side corresponding to the vertical component of magnetic tension may be written as

$$\boldsymbol{B}_h \cdot \nabla B_z = B_h^2 \frac{1}{R_B}\,, \tag{11}$$

where R_B is the radius of curvature of field line measured in the vertical direction. If the field line near the point of interest is concave upward (downward), R_B is positive (negative). With the introduction of magnetic scale height

$$H_B \equiv -\left(\frac{\partial \ln B_h}{\partial z}\right)^{-1} \tag{12}$$

and a positive-definite dimensionless parameter

$$\alpha_B \equiv \frac{B_h^2}{4\pi p}\,, \tag{13}$$

equation (10) can be recast into the form

$$\frac{1}{H_s} = \frac{1}{H_p} + \alpha_B\left[\frac{1}{H_B} + \frac{1}{R_B}\right]\,. \tag{14}$$

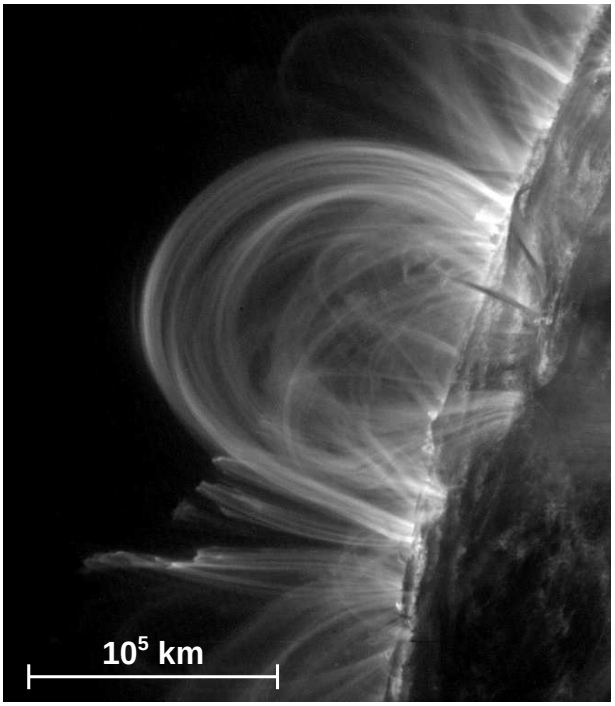

Fig. 3.— Coronal loops emitting EUV light at 171 Å. The image was taken by the *Transition Region And Coronal Explorer*.

The condition for non-hydrostatic support as expressed in equation (6) is satisfied if $\alpha_B \neq 0$ and

$$\frac{1}{H_B} + \frac{1}{R_B} > 0\,, \tag{15}$$

which implies that magnetic field should differ from the force-free field satisfying the condition

$$\frac{1}{H_B} + \frac{1}{R_B} = 0\,, \tag{16}$$

for magnetic support to operate.

A special case of magnetic support arises when $1/H_p = 1/H_B = 0$: non-hydrostatic support purely by the force of magnetic tension

$$\frac{1}{H_s} = \frac{\alpha_B}{R_B}\,. \tag{17}$$

The famous solution of Kippenhahn & Schlüter (1957) for a magnetohydrostatic equilibrium belongs to this category.

2.4 Dynamical Support

Suppose magnetic field does not contribute to non-hydrostatic support at all, and the plasma is not static. The hydrostatic equation is then replaced by the vertical component of the equation of motion

$$\rho g = -\frac{\partial p}{\partial z} - \rho a_z\,, \tag{18}$$

with vertical acceleration a_z given by

$$a_z = \frac{\partial v_z}{\partial t} + \boldsymbol{v}\cdot\nabla v_z\,. \tag{19}$$

This equation may be rewritten in terms of scale heights

$$\frac{1}{H_s} = \frac{1}{H_p} - \frac{a_z}{g}\frac{1}{H_s}\,, \tag{20}$$

which indicates that the dynamical support of non-hydrostatic plasma operates when

$$a_z < 0\,. \tag{21}$$

This is not surprising at all; since the force of plasma pressure gradient can not balance the force of gravity and there is no other force, the plasma should be subject to a net vertical acceleration downward.

The point is that whether the non-hydrostatic support has a dynamical origin or not can be decided based on the value of vertical acceleration. If the dynamical support is the only way of non-hydrostatic support, the acceleration should be close to the theoretical one given by

$$a_z = g(\frac{H_s}{H_p} - 1)\,. \tag{22}$$

Since non-hydrostatic support implies that H_s/H_p is significantly smaller than unity, a_z should be a significant fraction of $-g$. The extreme case of free-fall $a_z = -g$ corresponds to the case of $H_s/H_p = 0$ in which case hydrostatic support by pressure gradient is negligible.

Once a constant value of a_z is assumed, it is easy to investigate the observable characteristics of dynamical support from the solution of equation of motion:

$$v_z = a_z t \tag{23}$$

and

$$z = \frac{1}{2}a_z t^2 \tag{24}$$

where time t and height z are measured from the instant when, and the position where the vertical speed becomes zero. The $h \equiv |z|$ may be interpreted as the vertical extent of the non-hydrostatic structure; $\tau \equiv 2|t|$, as the dynamic lifetime of the structure and $v_m \equiv |a_z t|/2$, the average vertical speed of the structure. Then we obtain the following relations for τ

$$\tau = \sqrt{8h/|a_z|} \tag{25}$$

and v_m

$$v_m = \sqrt{|a_z|h/2} \tag{26}$$

expressed in terms of a_z and h. For example, if we choose $h = 10^4$ km and $|a_z| = g$, we find that $\tau = 9$ min and $v_m = 37$ km s^{-1}.

The consideration above followed the Lagrangian approach in which case it does not matter whether motion

is steady or not. As a matter of fact, one can derive the same expressions for a purely vertical steady flow with a constant vertical acceleration as well, by integrating the equation

$$a_z = v_z \frac{\partial v_z}{\partial z} . \tag{27}$$

What would be the effect of steady horizontal flows on dynamical support? To see this, we consider the case

$$a_z = \boldsymbol{v}_h \cdot \nabla v_z = v_h \frac{\partial v_z}{\partial x} \tag{28}$$

with constant a_z, constant $\boldsymbol{v}_h$, and $v_z = 0$ at $x = 0$. The integration of this equation results in

$$v_z = \frac{a_z}{v_h} L , \tag{29}$$

where L is the horizontal displacement from $x = 0$. For the flow to remain predominantly horizontal, it should hold

$$v_h \gg \sqrt{|a_z| L} \tag{30}$$

and hence

$$\tau_h \equiv \frac{2L}{v_h} \ll 2\sqrt{L/|a_z|} , \tag{31}$$

where τ_h is the duration of the period during which the flow can remain predominantly horizontal.

There are a couple of characteristics we can infer from these conditions. First, purely horizontal flows have nothing to do with dynamical support: they need some forces to balance the force of gravity anyway. In the dynamical support, it is natural for a flow to follow a curved trajectory that is concave downward. Second, the necessary condition for the flow to remain predominantly horizontal is that the speed of horizontal motion should be high enough. For example, with the choice of $L = 10^5$ km, and $|a_z| = g$, we obtain the specific conditions: $v_h \gg 165$ km s^{-1}, and $\tau_h \ll 20$ min.

2.5 General Non-Hydrostatic Support

In general, both magnetic support and dynamical support may be responsible for the hon-hydrostatic support, as can be expressed in the equation

$$\frac{1}{H_s} = \frac{1}{H_p} + \alpha_B \left[\frac{1}{H_B} + \frac{1}{R_B} \right] - \frac{a_z}{g} \frac{1}{H_s} \tag{32}$$

or

$$\frac{1}{H_s} = \left(\frac{1}{H_p} + \alpha_B \left[\frac{1}{H_B} + \frac{1}{R_B} \right] \right) \left(1 + \frac{a_z}{g} \right)^{-1} . \tag{33}$$

Note that this equation is equivalent to the vertical component of equation of motion in ideal MHD, being written in terms of scale lengths and dimensionless parameters whereas the original equation of motion is written in terms of physical variables p, ρ, $\boldsymbol{v}$, $\boldsymbol{B}$ and their spatial gradients. We think it is convenient to work with scale lengths since these are good measures of the spatial variations of the physical parameters and may be inferred from observations more easily than the physical parameters themselves. Moreover, the other lengths such as h and L introduced above can be directly determined from observations.

The general condition for non-hydrostatic support now reads

$$-\frac{a_z}{g} + \alpha_B \left(\frac{H_s}{H_B} + \frac{H_s}{R_B} \right) > 0 , \tag{34}$$

from which it is obvious that if $\alpha_B = 0$ (zero horizontal magnetic field), it should follow $a_z < 0$; the plasma should move with a *downward* acceleration (dynamical support). On the other hand, if $a_z = 0$ (static or constant motion), it should follow $\alpha_B \neq 0$; there should exist significant *horizontal* magnetic fields with a suitable configuration (magnetic support). To decide between the two ways of non-hydrostatic support, it is crucial for one to determine the vertical acceleration of a non-hydrostatic feature.

3. MEASUREMENTS OF PARAMETERS

In principle, the way of non-hydrostatic support can be fully understood based on the quantitative evaluation of dynamical support and magnetic support if the parameters H_s, H_p, a_z, H_B, R_B, and α_B are determined from observations.

3.1 Hydrostatic Scale Height

Hydrostatic pressure scale height H_s depends on temperature T, mean molecular weight μ, and gravity g. Even though the precise determination of T and μ from observations is not a trivial task, rough estimates can be readily obtained once the spectral window is specified. For example, chromospheric features well visible through the Hα line should contain enough number of neutral hydrogens (hydrogen should be either neutral or partially ionized), which suggests $T \sim 10^4$ K and $\mu \sim 1$, and hence $H_s \sim 300$ km. On the other hand, coronal features well visible through a filter centered either on 171 Å or 195 Å must be fully ionized plasma with $T \sim 10^6$ K, and $\mu \sim 0.6$, so it follows that $H_s \sim 50,000$ km.

3.2 Pressure Scale Height

The determination of pressure scale height H_p is a little difficult. In principle, it is necessary to determine temperature, mass density, mean molecular weight as functions of height, to obtain the height dependence of pressure from which H_p can be determined. This requires a detailed analysis of density diagnostic at different heights.

The scale height of a feature H_f can be directly, if not precisely, measured from the variation of intensity. We find it possible to relate H_f to H_p using some

simplifying assumptions suitable in each situation. For instance, a spicule beyond the limb emits the Hα radiation mainly by scattering the light illuminated from the photosphere. If the spicule is optically thin across, the intensity should be proportional to the optical thickness across it. Supposing that diameter and temperature are uniform along the spicule, H_f inferred from the intensity variation along the spicule is found to be the same as that of pressure variation H_p. Thus H_p in this case is roughly the height over which intensity is reduced to $e^{-1} \approx 0.37$ of the original value. In contrast, a coronal loop emits the EUV radiation mainly by collisional excitation followed by radiative de-excitation. Supposing again that diameter and temperature are uniform along the loop, the intensity variation along the loop reflects the variation of square of electron and hence that of the square of pressure, so that we have the relation $H_f = H_p/2$. In other words, H_p is roughly the height over which the intensity is reduced by a factor of $e^{-2} \approx 0.14$.

3.3 Dynamical Parameters

The determination of vertical acceleration a_z is one of the observational challenges in the solar research. By decomposing the acceleration vector $\boldsymbol{a}$ into the line-of-sight component $a_l\hat{l}$ and the transverse component $a_t\hat{t}$, we can express a_z as

$$a_z = \boldsymbol{a} \cdot \hat{z} = a_t\hat{t} \cdot \hat{z} + a_l\hat{l} \cdot \hat{z} \,. \tag{35}$$

In principle, we can determine a_t from the analysis of a time series of images, and a_l from a time series of Doppler shifts of a spectral line.

When there exists a prominent discrete feature on the images, its position can be tracked as a function of time using optical flow techniques such as the well-known local correlation tracking (LCT, November & Simon 1988) or its improved version, non-linear affine velocity estimator (NAVE, Chae & Sakurai 2008). The output of these techniques is position vector, its time derivative (velocity vector), and its second time derivative (acceleration vector $a_t\hat{t}$) on the plane of sky. If the feature linearly moves toward a direction $\hat{t}$, the time-slice technique is quite conveniently used. This technique stacks a time series of thin stripes each of which is taken along a designated line in each image, and produces a map of intensity in the time-distance domain. This map is useful in displaying the position of the feature as a function of time, from which one can derive velocity and acceleration a_t along the direction $\hat{t}$.

The component of acceleration along the line of sight a_l can be determined from a time variation of Doppler shift of a spectral line emitted by the feature. When the spectral line is in emission, the Doppler shift can be determined from the central wavelength of the line without much difficulty. But when the spectral line is in absorption as in the case of Hα disk observations of chromospheric features, the central wavelength of the line should not be used for the Doppler shift. This is because the line is mostly formed in the photosphere, and the chromospheric feature observed through the line modifies the spectral shape of the line only a little. The central wavelength of the line measures the weighted average of the line-of-sight velocity of the photosphere and the line-of-sight velocity of the chromospheric feature with the chromospheric weight being much smaller than the photospheric weight. One should rather determine the line-of-sight velocity of the chromospheric feature from the central wavelength of the absorption profile of the feature after taking into account the effect of radiative transfer through the chromospheric feature on the observed line profile. One simple approach is to adopt the cloud model of radiative transfer where the source function and other parameters are assumed to be constant inside the chromospheric feature. For the details of this issue, readers may refer to Chae et al. (2006).

Note that knowing a_t and a_l is not enough for the determination of a_z. The orientation of the z-axis should be determined somehow so that the values of $\hat{t} \cdot \hat{z}$ and $\hat{l} \cdot \hat{z}$ can be specified.

In many cases, it is much more difficult to determine the vertical acceleration a_z than to do the vertical velocity v_z, since the determination of a_z requires the knowledge of the time variation of v_z. When the information on the time variation of v_z is not available, one can infer a_z roughly from the typical vertical speed v_m and the vertical extent of motion h using equation (26).

3.4 Magnetic Parameters

The direct determination of magnetic field in the upper solar atmosphere is quite demanding. The recent progress in the analysis of the Hanle effect on the polarization of light at the wavelengths in the spectral lines opened the door to the measurement of vector magnetic field in chromospheric features that lie much above the limb such as prominences (López Ariste & Casini 2003; Casini et al. 2009) and spicules (López Ariste and Casini 2005). Being combined with the high resolving capability of the new generation telescopes, this technique will provide a good opportunity for investigating the magnetic structures of prominence and spicules sooner or later. The inference of magnetic structures of other chromospheric features is more difficult, and may not be possible in the near future. Limb observations are not good at resolving individual structures, and disk observations are difficult to analyze because of strong and non-uniform illuminating light from below.

The direct determination of coronal magnetic field is extremely demanding. The Zeeman effect on the spectral lines in the UV and visible wavelengths can not be made use of to determine coronal field since the Doppler broadening dominates over the Zeeman splitting in these lines. Instead, near-infrared coronal emission lines can be used to measure the polarization

resulting from the Zeeman effect (Lin et al. 2000), or gyro-resonance radio emission can be used to directly infer the field strength (Lee 2007). The measurement of coronal magnetic field is one of the major scientific goals of the next generation telescope such as the Advanced Technology Solar Telescope (Keil et al. 2003).

Despite the fast development of solar observing instrumentation, it would not be possible to obtain the magnetic parameters of our interest directly from observations for a while. What we need is much more than the average value of the total field strength only; we need to obtain the horizontal field strength, and its vertical scale height, and its radius of curvature in the vertical direction.

4. CURRENT UNDERSTANDING OF NON-HYDROSTATIC FEATURES

4.1 Spicules and Dynamic Fibrils

Spicules seen beyond the limb of quiet regions, mottles seen on quiet regions on the disk, and dynamic fibrils seen in active regions on the disk are qualitatively very similar to one another. Observations have provided ample evidence that these features are mainly dynamically supported against gravity. The most compelling evidence is that the top of each feature usually moves up and falls back along a line with a constant deceleration that is a significant fraction of gravity (Suematsu et al. 1995; Christopoulou et al. 2001; De Pontieu et al. 2007). That the deceleration is smaller than that of gravity was usually explained by supposing the line of motion is inclined from the vertical direction whereas most studies implicitly neglected the effect of pressure gradient on the dynamics.

We pay special attention to the reported values of dynamic lifetime because their measurements are independent of the perspective of the observer. The reported mean lifetimes of spicules are 7 min from limb observations (Pasachoff et al. 2009), and 10 min from disk observations (Suematsu et al. 1995). It appears to us that the lifetimes measured by Suematsu et al. (1995) may have been overestimated since they measured the distance from the location where the ballistic motion of the feature is not identified. If we confine the identification of the feature to the period of time when the ballistic motion is clear, we find from Fig. 4 of their paper that the lifetime should be decreased by a factor of about 1.4, which gives about the same value of the mean lifetime as that of limb spicules reported by Pasachoff et al. (2009). This value is equal to the theoretical lifetime determined from equation (25) with $a_z = -g$ and $h = 6,000$ km. This choice of h is quite consistent with the observed range of spicule heights (Pasachoff et al. 2009). Interestingly, the mean value calculated using equation (26) with the same parameters is found to be 29 km s^{-1}, which is again very close to the mean value of 27 km s^{-1} reported by Pasachoff et al. (2009). These results strongly support the notion that spicules are dynamically supported.

4.2 Prominences

Even though prominences traditionally refer to all the cool features that appear prominent, especially in Hα, above the chromospheric layer outside the solar limb, we restrict the usage of this terminology to the Hα features outside the limb that correspond to dark filaments seen on the solar disk. There are a variety of prominences on the Sun. Depending on the activity, prominences may be classified into eruptive prominences or quiescent prominences. Depending on the photospheric region of location, prominences may be classified into active region prominences, quiet region prominences, or intermediate prominences.

Quiescent prominences are an extreme example of non-hydrostatic support in that they represent cool plasma lying much above the chromosphere, not to speak of the photosphere. They apparently keep stable for relatively long periods as long as many days, so that it has been thought that quiescent prominences are static, and a number of prominence models (e.g., Kippenhahn & Schlüter 1957; Kuperus & Raadu 1974) have been proposed to explain the magnetic configuration necessary for the magnetic support of plasma against the force of gravity.

This traditional picture of magnetic support, however, is now being challenged by recent observations of fine-scale structures in prominences that reported the common occurrence of flows. The primary advocate is Zirker et al. (1998) who argued that their finding of Hα flows streaming along threads not only in the spine, the upper horizontal portion of a filament, but also in in the barbs, the lower portions looking like legs, is evidence against the presence of horizontal magnetic fields that are essential for magnetic support. The speeds of the reported flows were from 5 to 20 km s^{-1}, and the distances tracked, from 10^3 to 10^4 km. Soon thereafter, Wang (1999) reported flows with higher speeds of order 30 km s^{-1} from He II λ304 images, and regarded prominences as a system of chromospheric jets, a dynamic entity. Since then, there has been accumulating evidence for streaming flows in Hα (Chae et al. 2000; Lin et al. 2003, 2005; Chae et al. 2007, 2008) and in EUV (Chae 2003; Kucera et al. 2003).

Could the existence of streaming flows be used as evidence against magnetic support, and for dynamical support in prominences, as Zirker et al. (1998) suggested? We think not. The reason is quite simple: the speeds of observed flows are too low. If magnetic support does not operate at all, and plasmas are wholly dynamically supported, then the speed should be consistent with equation (26) in case of vertical flows and with equation (30) in case of horizontal flows. Based on the picture given by Zirker et al. (1998), we can reasonably choose $h = 15,000$ km, and $L = 50,000$ km, which leads to $v_m = 45$ km s^{-1} as the theoretical estimate of the mean speed of flows in the barbs, and $v_h \gg 120$

km s^{-1} for the speed of flows in the spine. These speeds are much higher than the observed speeds: 5 km s^{-1} in the barbs, and 20 km s^{-1} in the spine, respectively. No Hα observations have ever reported such high speed flows so far. It seems that at least Hα emitting plasmas in prominences should be magnetically supported, and the existence of streaming flows does not negate such need.

Flows may be important in prominences from the veiwpoint of mass supply and its redistribution (Litvinenko & Martin 1999; Chae 2003), but their relevant dynamics should be understood in the framework of a moderate deviation from a magnetohydrostatic equilibrium, with the notion of magnetic support not being totally thrown away (Litvinenko 2000). Chae (2010) demonstrated that this conclusion holds for descending motions of knots as well that are often seen in hedgerow prominences.

4.3 General Chromosphere

Hα centerline images of the limb show a fairly continuous emitting band about 5,000 km high, in addition to spicules (see Fig. 1). Zirin (1988, 1996) argued that this "general chromosphere" is distinct from the spicule forest since it is not visible near the Hα offband at which spicules are most conspicuous. The Hα brightness scale height of the general chromosphere is of order 1,000 km, and the CICM model (Ewell et al. 1993) constructed from eclipse observations at a submillimeter wavelength indicates a pressure scale height of about 500 km, and an electron scale height of 1,000 km. These results strongly suggest that the general chromosphere is not in hydrostatic equilibrium, unlike the widely used VAL model (Vernazza et al. 1981) that yields 2,000 km for the height of chromosphere. The solar chromosphere requires non-hydrostatic support. So far, however, few studies have been done on this issue.

We agree with Zirin (1996) that the non-hydrostatic support of the general chromosphere is magnetic in nature. The reason is that the general chromosphere is not likely to be moving at fast speeds, as can be inferred from the observational fact that the general chromosphere is more conspicuous at the Hα center than at offbands, unlike spicules.

Zirin (1996) attributed this component to intranetwork regions in which spicules are absent, and he identified the general chromosphere with the "intranetwork" chromosphere. We, however, think about the general chromosphere in a little different way. We recall that for magnetic support to operate, not only magnetic fields are required, but also the fields should be significantly horizontal. We also note that magnetic field may be significantly horizontal at regions where field lines connect to poles of opposite polarity. Such magnetic loops should be small enough to be confined inside the chromospheric layer of 5,000 km height. Thus we propose that the general chromosphere is supported by numerous magnetic loops with footpoint separation of 10^4 km or smaller. These loops may include magnetic bipoles inside intranetwork regions, and hence the general chromosphere should include the intranetwork chromosphere as well.

4.4 Coronal Loops

According to Aschwanden et al. (2000), some coronal loops visible in EUV have very large pressure scale height indicating the value of H_p/H_s as large as 3, requiring non-hydrostatic support. Suppose these loops are dynamically supported. With the choice of $h = 10^5$ km and $a_z = -g$, equation (26) indicates that the mean vertical speed should be about 120 km s^{-1}. Flows as fast as this value have not been observed in quiescent loops, even though downflows as fast as 40 km s^{-1} were reported (Winebarger et al. 2002). Therefore the non-hydrostatic support of coronal loops can not be explained by dynamic support in a vertical field. A similar conclusion was reached by Petrie (2006) as well.

The inadequacy of dynamical support of the non-hydrostatic loops leaves magnetic support as the only possibility. This obvious conclusion has a crucial physical implication: coronal loops should have horizontal magnetic fields. This requirement is not compatible with the common picture that identifies a coronal loop with an untwisted flux tube. Thus the implied magnetic support suggests us to reconsider the magnetic configuration of coronal loops; either the flux tube may be twisted or a totally different magnetic configuration may be required. This necessity arises also from another unresolved problem of how coronal loops can keep more or less constant width, despite the inferred expansion of a flux tube with height (Watko & Klimchuk 2000).

Recently, Plowman et al. (2009) identified the axis of coronal loops with field lines called separators and found that the observed coronal loop expansion properties can be well explained. We think that this is an interesting idea from the viewpoint of magnetic support as well, because magnetic fields in the immediate regions surrounding a separator should have significant components perpendicular to the separator itself. This means that even when the axis of a coronal loop is vertical along a separator, the non-axis part of the loop can be permeated by magnetic fields that are significantly horizontal. Therefore we propose that such a configuration can provide magnetic support. A rigorous theoretical investigation of this aspect is quite worthwhile.

5. SUMMARY AND CONCLUSION

The existence of plasma structures at altitudes much above hydrostatic scale heights suggests that these structures are not in hydrostatic equilibrium; the force of plasma pressure gradient is not strong enough to balance the force of gravity, and hence these structures need non-hydrostatic support. We find that the physics of non-hydrostatic support is relatively simple and can

be fairly well understood using the modified form of the vertical component of equation of motion. With the assumption of ideal MHD, the Lorentz force is the only force other than the force of plasma pressure gradient that can balance the force of gravity. Therefore there are basically two possibilities of non-hydrostatic support: either the system is not static at all (dynamical support) or the Lorentz force balances the force of gravity (magnetic support). Whether a non-hydrostatic plasma structure is dynamically supported or not can be determined using the value of vertical acceleration; if the vertical acceleration is downward and its magnitude is a significant fraction of the gravitational acceleration, the structure is far from a static equilibrium and is dynamically supported. If not, the structure must be in a magnetohydrostatic equilibrium where the magnetic force balances the force of gravity. An obvious, but important property of magnetic support is that there should exist significant horizontal components of the magnetic fields.

We have considered the physical nature of non-hydrostatic support in each of the several kinds of non-hydrostatic structures using observational results previously reported. Observations seem to be quite consistent with the notion that spicules in quiet regions and dynamic fibrils in active regions are dynamically supported. This means that these structures are a dynamical consequence of initial supply of enough vertical momentum in low altitudes. How they come to have such momentum is another issue and is actually the heart of research on these structures. On the other hand, the general chromosphere as well as prominences seems to be magnetically supported and they should be pervaded by horizontal magnetic fields. The presence of flows in prominences does not necessarily mean that these structures are dynamically supported. Non-hydrostatic support of plasmas in cool coronal loops emitting EUV does not seem to be dynamic in nature, either. If this is the case, magnetic support is required even for coronal loops and a magnetic configuration other than a simple magnetic flux tube is required to be consistent with the implied existence of significant horizontal components of magnetic fields.

We conclude that considering the non-hydrostatic aspect of plasma structures in the solar chromosphere and corona is helpful in understanding their magnetic structures and relevant physical processes. The physics of non-hydrostatic support is so simple as to be easily made use of, which gives us a strong motivation to properly measure physical quantities such as scale heights, dynamical parameters, and magnetic parameters using the coming advanced observations, and combine them to make a consistent picture.

ACKNOWLEDGMENTS

This work was supported by the National Research Foundation of Korea (KRF-2008-220-C00022).

APPENDIX A. Derivation of Eq. (11)

Let's denote magnetic field at the point of interest $\boldsymbol{r}_0$ by

$$\boldsymbol{B}_0 = B_{h0}\hat{x} + B_{z0}\hat{z} \tag{A1}$$

where $\hat{h}$ is the direction vector of the horizontal component. The line of field $\boldsymbol{b} \equiv \boldsymbol{B} - B_{z0}\hat{z}$ is then horizontal at $\boldsymbol{r}_0$. Unless purely horizontal, this line of field near $\boldsymbol{r}_0$ may be fitted by a circle with a radius, say, R_B. We choose the convention that R_B is positive if the field line is concave upward. A position on the circle is specified by the position angle θ that is measured counterclockwise and hence is related to the horizontal coordinate h in the way the relation

$$h = R_B \sin\theta \tag{A2}$$

and the behavior of $\boldsymbol{b}$ in the neighborhood of the point of interest $\boldsymbol{r}_0$ is described by the relations

$$b_h = B_{h0}\cos\theta \tag{A3}$$
$$b_z = B_{h0}\sin\theta\,. \tag{A4}$$

Thus we have

$$\boldsymbol{B}_h \cdot \nabla B_z = b_h \frac{\partial b_z}{\partial h} = B_{h0}^2 \frac{1}{R_B}\cos\theta \tag{A5}$$

which is reduced to

$$\boldsymbol{B}_h \cdot \nabla B_z = B_h^2 \frac{1}{R_B} \tag{A6}$$

in the limit $\theta \to 0$ corresponding to the point of our interest $\boldsymbol{r}_0$.

REFERENCES

Aschwanden, M. J., Nightingale, R. W., & Alexander, D. 2000, Evidence for Nonuniform Heating of Coronal Loops Inferred from Multithread Modeling of TRACE Data, ApJ, 541, 1059

Aschwanden, M. J., Schrijver, C. J., & Alexander, D. 2001, Modeling of Coronal EUV Loops Observed with TRACE. I. Hydrostatic Solutions with Nonuniform Heating, ApJ, 550, 1036

Casini, R., López Ariste, A., Paletou, F., & Léger, L. 2009, Multi-Line Stokes Inversion for Prominence Magnetic-Field Diagnostics, ApJ, 703, 114

Chae, J., Denker, C., Spirock, T. J., Wang, H., & Goode, P. R. 2000, High-Resolution Hα Observations of Proper Motion in NOAA 8668: Evidence for Filament Mass Injection by Chromospheric Reconnection, Sol. Phys., 195, 333

Chae, J. 2003, The Formation of a Prominence in NOAA Active Region 8668. II. Trace Observations of Jets and Eruptions Associated with Canceling Magnetic Features, ApJ, 584, 1084

Chae, J., Park, Y.-D., & Park, H.-M. 2006, Imaging Spectroscopy of a Solar Filament Using a Tunable Hα Filter, Sol. Phys., 234, 115

Chae, J., Park, H.-M., & Park, Y.-D. 2007, Hα Spectral Properties of Velocity Threads Constituting a Quiescent Solar Filament, JKAS, 40, 67

Chae, J., Ahn, K., Lim, E.-K., Choe, G. S., & Sakurai, T. 2008, Persistent Horizontal Flows and Magnetic Support of Vertical Threads in a Quiescent Prominence, ApJ, 689, L73

Chae, J., & Sakurai, T. 2008, A Test of Three Optical Flow Techniques-LCT, DAVE, and NAVE, ApJ, 689, 593

Chae, J. 2010, Dynamics of Vertical Threads and Descending Knots in a Hedgerow Prominence, ApJ, in press

Christopoulou, E. B., Georgakilas, A. A., & Koutchmy, S. 2001, Fine Structure of the Magnetic Chromosphere: Near-Limb Imaging, Data Processing and Analysis of Spicules and Mottles, Sol. Phys., 199, 61

De Pontieu, B., Hansteen, V. H., Rouppe van der Voort, L., van Noort, M., & Carlsson, M. 2007, High-Resolution Observations and Modeling of Dynamic Fibrils, ApJ, 655, 624

Ewell, M. W., Jr., Zirin, H., Jensen, J. B., & Bastian, T. S. 1993, Submillimeter Observations of the 1991 July 11 Total Solar Eclipse, ApJ, 403, 426

Foukal, P. 1971, Hα Fine Structure and the Chromospheric Field, Sol. Phys., 20, 298

Johannesson, A., & Zirin, H. 1996, The Pole-Equator Variation of Solar Chromospheric Height, ApJ, 471, 510

Keil, S. L., & 10 colleagues 2003, Design and development of the Advanced Technology Solar Telescope (ATST), Society of Photo-Optical Instrumentation Engineers (SPIE) Conference Series, 4853, 240

Kippenhahn, R., & Schlüter, A. 1957, Eine Theorie der solaren Filamente. Mit 7 Textabbildungen, Zeitschrift fur Astrophysik, 43, 36

Kucera, T. A., Tovar, M., & De Pontieu, B. 2003, Prominence Motions Observed at High Cadences in Temperatures from 10 000 to 250 000 K, Sol. Phys., 212, 81

Kuperus, M., & Raadu, M. A. 1974, The Support of Prominences Formed in Neutral Sheets, A&A, 31, 189

Lee, J. 2007, Radio Emissions from Solar Active Regions, Space Science Reviews, 133, 73

Lin, H., Penn, M. J., & Tomczyk, S. 2000, A New Precise Measurement of the Coronal Magnetic Field Strength, ApJ, 541, L83

Lin, Y., Engvold, O. R., & Wiik, J. E. 2003, Counterstreaming in a Large Polar Crown Filament, Sol. Phys., 216, 109

Lin, Y., Engvold, O., Rouppe van der Voort, L., & Wiik, J. E., Berger, T. E. 2005, Thin Threads of Solar Filaments, Sol. Phys., 226, 239

Lippincott, S. L. 1957, Chromospheric Spicules, Smithsonian Contributions to Astrophysics, 2, 15

Litvinenko, Y. E., & Martin, S. F. 1999, Magnetic Reconnection as the Cause of a Photospheric Canceling Feature and Mass Flows in a Filament, Sol. Phys., 190, 45

Litvinenko, Y. E. 2000, On the Magnetic Field Orientation and Plasma Flows in Solar Filament Barbs, Sol. Phys., 196, 369

López Ariste, A., & Casini, R. 2003, Improved Estimate of the Magnetic Field in a Prominence, ApJ, 582, L51

López Ariste, A., & Casini, R. 2005, Inference of the Magnetic Field in Spicules from Spectropolarimetry of He I D3, A&A, 436, 325

November, L. J., & Simon, G. W. 1988, Precise Proper-Motion Measurement of Solar Granulation, ApJ, 333, 427

Pasachoff, J. M., Jacobson, W. A., & Sterling, A. C. 2009, Limb Spicules from the Ground and from Space, Sol. Phys., 260, 59

Petrie, G. J. D. 2006, Coronal Loop Widths and Pressure Scale Heights, ApJ, 649, 1078

Plowman, J. E., Kankelborg, C. C., & Longcope, D. W. 2009, Coronal Loop Expansion Properties Explained Using Separators, ApJ, 706, 108

Suematsu, Y., Wang, H., & Zirin, H. 1995, High-Resolution Observation of Disk Spicules. I. Evolution and Kinematics of Spicules in the Enhanced Network, ApJ, 450, 411

Vernazza, J. E., Avrett, E. H., & Loeser, R. 1981, Structure of the Solar Chromosphere. III - Models of the EUV Brightness Components of the Quiet-Sun, ApJS, 45, 635

Wang, Y.-M. 1999, The Jetlike Nature of HE II Lambda304 Prominences, ApJ, 520, L71

Watko, J. A., & Klimchuk, J. A. 2000, Width Variations along Coronal Loops Observed by TRACE, Sol. Phys., 193, 77

Winebarger, A. R., Warren, H., van Ballegooijen, A., DeLuca, E. E., & Golub, L. 2002, Steady Flows Detected in Extreme-Ultraviolet Loops, ApJ, 567, L89

Zirin, H. 1988, Astrophysics of the sun, Cambridge and New York, Cambridge University Press

Zirin, H. 1996, The Mystery of the Chromosphere, Sol. Phys., 169, 313

Zirker, J. B., Engvold, O., & Martin, S. F. 1998., Counter-Streaming Gas Flows in Solar Prominences as Evidence for Vertical Magnetic Fields, Nature, 396, 440